
Article:
Galanakis, N. and Travis, K.P. orcid.org/0000-0001-8557-2689 (2017) A new order parameter based method for characterizing radiation damage in amorphous materials. Langmuir, 33 (42). pp. 11825-11833. ISSN 0743-7463

https://doi.org/10.1021/acs.langmuir.7b02649

A New Order Parameter Based Method for Characterizing Radiation Damage In Amorphous Materials

Nikolaos Galanakis* and Karl P. Travis

Department of Materials Science & Engineering, University of Sheffield, Sir Robert Hadfield Building, Sheffield, S1 3JD, UK

E-mail: ngalanakis1@sheffield.ac.uk

Abstract

We present a new method of characterizing damage arising from α-recoil cascades in amorphous materials including glasses. The approach taken is topological, yielding information of atom connectivity and utilising complete sets of orthogonal functions (spherical harmonics and Hermite functions) to compute order parameters.

The utility of our new approach is demonstrated by first applying it to models of radiation damaged crystalline zircon, enabling validation against the standard defect counting method (Wigner-Seitz). We then apply it to a simple model of a glass, obtained by supercooling a Lennard-Jones liquid, for which defect counting methods are inapplicable.

The method shows great promise for use in characterizing damage in more complicated glasses, particularly those of interest in immobilisation of nuclear waste and when used in conjunction with non-equilibrium computer simulation, could be a powerful tool to elucidate experimental data on radiation tolerance of such wasteforms.

*To whom correspondence should be addressed

Introduction

In the UK and countries including France, Russia and India, high level nuclear waste (HLW) is immobilized through a process known as vitrification. This process entails calcination of the liquid waste, followed by melting the calcined wastes with a mixtures of glass frit and various additives to control the final properties of the solid glass but also to control its viscosity while molten. The molten mixture is then poured into stainless steel containers, which are subsequently sealed and placed in dry storage, awaiting final disposal. Glass is the preferred wasteform for HLW largely because of its chemical flexibility - it can incorporate a large range of atomic species within the matrix. However, one of the disadvantages is a low chemical durability. Self-irradiation from elements within the matrix, particularly alpha decay cascades, can lead to loss of local structure, ultimately causing devitrification and failure of the wasteform. Understanding the effects of alpha recoil cascades in amorphous materials is a key step towards developing more durable and safer glass wasteforms.

Numerical modeling has emerged as a powerful tool to assist experimental studies of the effects of radiation damage in wasteforms. Alpha cascades can be directly followed in real time using non-equilibrium molecular dynamics in which an atom is selected as the primary knock-on atom (PKA) and given an additional component of kinetic energy over and above that due to thermal motions. The development of point defects, the propagation of damage and any subsequent recovery can then be observed for a timescale typically up to 100 picoseconds at the atomic scale using classical forcefields and large system sizes. By simulating damage in families of related materials, the numerical work can guide experimental programmes by reducing the list of candidate materials to be explored. Importantly, mechanistic information can be gleaned from computer experiments which is difficult or impossible to obtain using experiment alone.

Assuming that the classical forcefields (*ab initio* methods are presently restricted to small numbers of atoms and thus low recoil energies) used to construct models of the wasteforms are accurate, the results of *equilibrium* molecular simulations are essentially exact. However,

radiation damage modeling involves a non-equilibrium process and the results are sensitive to details such as heat removal (thermostatting), use of artificial boundary conditions (eg periodic boundary conditions) and the method used to characterize the damage. The method of characterizing damage is perhaps the most significant outstanding problem in radiation damage modeling. Traditional defect counting methods based on Wigner-Seitz cells are only suitable for crystalline materials in which there is a clear reference structure from which to compare against and thus enabling identification of point defects. Glasses, which are amorphous cannot be analysed using this method. However, even for crystalline materials, the Wigner-Seitz method is still problematic since the unit cell may distort significantly during a cascade - a fact not taken into account by the original method.[1] In addition the atoms of a glass are not in a state of thermodynamic equilibrium but instead undergo diffusive motion. In that case the Wigner-Seitz method would record a large number of false-positive damaged particles. For this reason, alternative methods based on topology have been developed and used. These methods include the use of Steinhardt order parameters,[2] ring statistics[3–10] and Maxwell constraint analysis.[11–14]

In all previous studies, Steinhardt order parameters (SOP) are used to obtain information regarding the structure of crystalline materials. However, none of these studies use SOP to provide information regarding the number of displaced particles. Moreover, with the exception of the work of Baranyai et al..[15] SOPs have not been applied to amorphous materials and particularly those used as nuclear wasteforms.

In this paper we report a new topological method of characterizing disorder arising from radiation damage based on an extension of Steinhardt order parameters but also including new order parameters based on Hermite functions. We validate our new method by considering radiation damaged crystalline zircon, in which the traditional defect counting method, though not perfect, provides the means to check the new method. We next apply the method to a simple model of a glass, namely the LJ glass, obtained by supercooling a LJ fluid. The method should be applicable to more complex glasses and other amorphous materials.

The paper is organized as follows. In the first section we describe the topological order parameters used in our method. In the second section we describe the models used and how they were prepared (crystalline zircon and LJ glass). In the third section we discuss the results obtained by applying the new method to crystalline and amorphous solids while in fourth section we discuss the usefulness of the method and indicate where it might be applicable.

Topological measures of disorder

Steinhardt order parameters

Common topological methods involve bond order parameters and Steinhardt order parameters. One of the uses of SOP was due to Baranyai et al..[15] These authors used SOP and more particularly the Q_ℓ vs ℓ bar charts for the first coordination cell of each atom to explore the differences in the structures of molten and glassy rubidium bromide. Lechner and Dellago[16] used SOP to study the structure of simple crystalline Lennard-Jones systems and a Gaussian core model, by investigating the distribution of Q_4 and Q_6 as well as their average values for all the atoms of the system. Unlike previous studies, Lechner and Dellago used both the first and the second coordination cell for their calculations. Reinhardt et al.[17] followed a similar approach to investigate ice nucleation in water models. A more sophisticated approach was followed by Archer et al.[2] in order to study the structure of pyrochlores for nuclear waste immobilization. These authors used two different cutoff distances for the calculation of the SOP. One with a small cutoff distance of 3.2 Å, to obtain global information, and a secondary cutoff distance of 12 Å to obtain information on local structures surrounding atoms.

Steinhardt Order Parameters[18] provide information regarding the angular distribution of the atoms of a system around a reference particle. One type of Steinhardt order parameter

is represented by the set of bond-orientational parameters defined by

$$\langle Q_{\ell,m}(\mathbf{r})\rangle = \frac{1}{N_b}\sum_{\mathrm{i}=1}^{N_b} Q_{\ell,m}(\mathbf{r}_i). \tag{1}$$

where N_b is the number of bonds for the reference particle and $Q_{\ell,m} = Y_\ell^m(\mathbf{r})$. $Y_\ell^m(\theta,\phi)$ are the complex spherical harmonic functions, defined by

$$Y_\ell^m(\theta,\phi) = (-1)^m\sqrt{\frac{2\ell+1}{4\pi}\frac{(\ell-m)!}{(\ell+m)!}}P_\ell^m(\cos\theta)e^{im\phi}, \qquad |m|\le\ell, \tag{2}$$

for integers ℓ and m, with the latter restricted to values between $-\ell$, $+\ell$, while $P_\ell^m(x)$ are associated Legendre polynomials defined by

$$P_\ell^m(x) = \frac{(-1)^m}{2^\ell\ell!}(1-x^2)^{m/2}\frac{d^{\ell+m}}{dx^{\ell+m}}(x^2-1)^\ell, \qquad m\ge 0, \tag{3}$$

$$P_\ell^m(x) = (-1)^m\frac{(\ell+m)!}{(\ell-m)!}P_\ell^{|m|}(x), \qquad m<0. \tag{4}$$

In the above equations, $\theta\in[0,\pi]$ and $\phi\in[0,2\pi]$ are the polar angle and azimuth of the spherical coordinate system. In the foregoing, the word "bond" is interpreted to mean the radius vector connecting a reference atom to one of its neighboring atoms lying within a sphere of specific radius, centered to the reference atom. Spherical harmonics for a given value of ℓ are members of the SO(3) rotational group that represents all the rotations in the 3D Euclidian space under the operation of composition. They are coordinate system dependent. To avoid this inconvenience the rotationally invariant term:

$$Q_\ell = \left[\frac{4\pi}{2\ell+1}\sum_{m=-\ell}^{\ell}|\langle Q_{\ell,m}(\mathbf{r})\rangle|^2\right]^{1/2}, \tag{5}$$

are also calculated. Since a radiation damage event will change the relative positions of the atoms of a system, it is expected to record this change in the values of SOP.

Hermite order parameters

The atoms of a crystalline solid occupy positions in the minima of the potential energy surface. Except at 0 K, these atoms vibrate about these equilibrium positions. The instantaneous bond vector connecting a reference atom to a given neighbor will change according to the vibrational motion of these atoms. Unless this motion is taken into account, misleading information could be obtained from SOP measures of radiation-induced disorder. A solution to this potential problem is as follows. Consider a reference particle i and the motion of an atom j at time t, described by the position vector $\mathbf{r}_{ij}(t)$, relative to its (0 K) position vector $\mathbf{r}_{ij,eq}(0)$ at the reference site. We can resolve this motion into a component parallel to this position vector:

$$r_{ij}^{\parallel}(t) = \mathbf{r}_{ij}(t) \cdot \mathbf{r}_{ij,eq}(0), \tag{6}$$

and a component perpendicular to it, defined by the equations:

$$\mathbf{r}_{ij}^{\perp}(t) \cdot \mathbf{r}_{ij,eq}(0) = 0, \tag{7}$$

$$\mathbf{r}_{ij}^{\perp}(t) \cdot [\mathbf{r}_{ij}(t) \times \mathbf{r}_{ij,eq}(0)] = 0, \tag{8}$$

$$|\mathbf{r}_{ij}^{\perp}(t)| = \frac{|\mathbf{r}_{ij}(t) \times \mathbf{r}_{ij,eq}(0)|}{r_{ij}(0)}. \tag{9}$$

The first equation ensures that the component is perpendicular to vector $\mathbf{r}_{i,eq}(0)$, the second that it lies at the same plane as vectors $\mathbf{r}_{i,eq}(0)$ and $\mathbf{r}_i(t)$ and the third that it has the appropriate length. Steinhardt order parameters are independent of the polar distance r and they actually ignore the movement of atom j which is parallel to the direction of $\mathbf{r}_{ij,eq}(0)$. SOP are only able to measure the rotational motion defined by vector $\mathbf{r}_{ij}^{\perp}(t)$. However, the motion captured by the parallel component is vibrational in nature and is more suitably represented by Hermite functions which emerge from the solution of the quantum mechanical oscillator. Hermite functions are sensitive to the displacement away from the equilibrium

position and they are able to record any alteration in the distance between two particles. This applies to the radiation damage situations where it is expected that Hermite functions will give information regarding the displacement of particles from their initial positions.

The Hermite functions are defined by

$$\psi_n(x) = (2^n n! \sqrt{\pi})^{1/2} H_n(x) e^{-x^2/2}, \qquad n = 0,\, 1,\, 2, \ldots \tag{10}$$

where $H_n(x)$ are the Hermite polynomials

$$H_n(x) = (-1)^n e^{x^2} \frac{d^n}{dx^n} e^{-x^2}, \qquad n = 0,\, 1,\, 2, \ldots \tag{11}$$

To enhance the effect of n and to be able the distinguish the different parameters, we define a set of modified Hermite functions, $\widetilde{\psi}_{nm}(x) = (x)$:

$$\widetilde{\psi}_{nm}(x) = (2^n n! \sqrt{\pi})^{1/2} H_n(x) e^{a_{nm} x^2/2}, \qquad n = 0,\, 1,\, 2, \ldots \tag{12}$$

in which $a_{nm} = n/n_m$ with n_m the largest value of n used in the calculations. These new functions retain the important orthogonality property, but are no longer normalized (this has no bearing on any of the results obtained).

Using the Hermite functions defined in eq. (12), we can construct a new order parameter which we shall henceforth refer to as a Hermite Order Parameter - HOP. By analogy with the SOPs, we define an average HOP by

$$\langle \widetilde{\psi}_n(r) \rangle = \frac{1}{N_b} \left[\sum_{\mathrm{i}=1}^{N_b} |\widetilde{\psi}_{nm}(r_i)|^2 \right]^{1/2}, \tag{13}$$

where the "bond" distance denoted by r in the above formula is obtained from the magnitude of the relative parallel vectors defined in eq. (6), between reference atom and its neighbor.

Model and force fields

Crystalline zircon

Zirconium silicate, commonly known as zircon, is a mineral with chemical formula $ZrSiO_4$ that crystallizes with the I41/amd space group. A significant amount of research has been devoted to molecular dynamics simulations of radiation damage in zircon (see for example Trachenko et al.[19–21] and Devanathan et al.[22]) which makes the modelling of radiation damaged zircon crystal quite straightforward. Apart from the study of radiation damage effects, these studies contributed to the establishment of reliable interatomic potentials for the zircon crystal.

A model for crystalline zircon consisting of a supercell of 5184 atoms was created using the DLPOLY 4 software package[23] (unit cell of 24 atoms). There are several different forcefields suitable for radiation damage modelling in zircon each with their own merits and disadvantages. In this work we have used one developed by Trachenko et al.[20] due to its ability to closely reproduce the structural properties of zircon, while simultaneously giving a reasonable estimate for the elastic constants.

The zircon forcefield consists of a Buckingham pairwise additive potential energy, $\phi(r)$, describing interactions between pairs of Zr-O and O-O atoms:

$$\phi_{\text{Buck}}(r) = Ae^{-r/\rho} - \frac{C}{r^6}. \tag{14}$$

with $r = |\mathbf{r}_{ij}|$; $\mathbf{r}_{ij} = \mathbf{r}_i - \mathbf{r}_j$, and parameters A, ρ and C are given in Table 1. For Si-O interactions, a Morse potential wa instead used:

$$\phi_{\text{Morse}} = D\left[e^{-2a(r-r_0)} - 2e^{-a(r-r_0)}\right]. \tag{15}$$

with values for the parameters D, a, r_0 also given in Table 1.

In addition to these contributions, a Coulombic term accounts for the electrostatic inter-

actions resulting from the partial charges assigned to the atomic species. The charges used for Zr, Si and O ions are +3.428, +1.356, and −1.196 respectively. The Coulombic contribution was evaluated using the Ewald summation method. In our simulations, we used an automatic parameter optimization for k-space provided by DLPOLY 4, and a real space cutoff of 25 Å. Once an initial superstructure had been created, it was relaxed using this forcefield through use of the energy minimization routine provided by the GULP software package.[24]

The energy-minimized structure previously described was equilibrated for a period of 10 ps at 300 K using NVT molecular dynamics. The temperature was controlled using a Langevin thermostat.

To create a damage cascade, a silicon particle (the primary knock-on atom, pka) is chosen near the centre of the supercell and given an additional quantity of kinetic energy equal to 4 keV over and above its thermal component. This kinetic energy defines the magnitude of the pka; its direction was selected such that its motion was directed along the [111] crystallographic direction. The high kinetic energy of the pka can create an extended and easily quantified damage cascade. However, the simultaneous use of periodic boundary conditions may allow energetic particles to travel through the periodic boundaries of the simulation box and either self-interact or create additional damage in regions of the simulation box that should not be affected by the radiation event. To prevent the energetic particles from traveling through the boundaries and re-entering the system during the non-equilibrium phase

Table 1: Parameters of the Buckingham and Morse potentials used for the zircon crystal model.

	Buckingham			Morse		
	A(eV)	ρ(Å)	C(eV·Å^6)	D(eV)	aÅ^{-1}	r_0(Å)
O-O	9245	0.2617	100	–	–	–
Zr-O	1477	0.317	0	–	–	–
Si-O	–	–	–	1.252	2.83	1.627

of the simulation, a Langevin boundary layer thermostat was applied at 300 K. Because of the small system size employed, the width of this boundary layer was taken to be 2 Å - the lowest possible value allowed by the DLPOLY 4 code. By examining the trajectories of the particles during the simulation, this boundary layer was proved sufficient to remove the excess of kinetic energy of the energetic particles and prevent them from traveling through the boundaries of the simulation box. A variable time step algorithm was applied that allowed the atoms of the system to travel a distance between 0.01 Å and 0.05 Å per time step, for 50,000 timesteps. The initial and the final timestep of the simulations was 0.01 fs and 0.1 fs respectively. The large kinetic energies involved in high energy cascades can lead to an increased possibility of smaller ionic separations that probe the divergent region of the Buckingham potential, giving rise to large (attractive) forces and unphysical clustering of similarly charged ion species. To avoid this, we have truncated the Buckingham potential for O-O interactions, replacing it at short distance with the ZBL potential,[25] joining the two smoothly with a cubic spline. The combined potential energy (not including the electrostatic contribution) is then defined piecewise by

$$\phi_{\text{O-O}}(r) = \begin{cases} \phi_{\text{ZBL}}(r), & r \leq r_{\text{ZBL}} \\ \phi_{\text{spline}}(r), & r_{\text{ZBL}} < r < r_{\text{Buck}} \\ \phi_{\text{Buck}}(r), & r \geq r_{\text{Buck}} \end{cases} \tag{16}$$

where $r_{\text{ZBL}} = 0.4$ Å and $r_{\text{Buck}} = 1.0$ Å.

Lennard-Jones glass

A LJ glass was constructed by supercooling a well-equilibrated LJ fluid following the method outlined in the paper by Rahman et al..[26] A LJ fluid was prepared by first constructing an

fcc lattice of 4000 atoms which are allowed to interact via the LJ pair potential

$$\phi_{\mathrm{LJ}}(r) = 4\epsilon \left[\left(\frac{\sigma}{r}\right)^{12} - \left(\frac{\sigma}{r}\right)^{6} \right], \tag{17}$$

where ϵ is the depth of the potential well and σ is the distance at which the potential is zero. The fcc lattice was constructed with a reduced number density, $\rho\sigma^3 = 0.95$. Using $\sigma = 3.4$ Å, this corresponds to a simulation cell length of 54.983 Å. The fcc structure then underwent a period of equilibration using DLPOLY 4 with a Nose-Hoover thermostat with set point temperature $T = 216$ K for 50,000 timesteps. The resulting fluid was then quenched using the same dynamics but now at $T = 12.96$ K to yield an amorphous solid LJ glass.

For the creation of the radiation damage cascade, an NVT Langevin thermostat was used with a boundary layer of 2 Å. The pka was given a kinetic energy of 0.2 eV and with a velocity direction chosen so that it traveled along the [111] crystallographic direction. The variable step algorithm was the same as for the simulation of the damage cascade in the zircon crystal and the simulation was run for 150,000 time steps.

Algorithmic details for defect analysis

The output of each simulation was recordered every 100 timesteps giving a total of 501 configurations (frames) to analyse, with one frame representing the initial undamaged structure, and the remaining 500 being the damaged structure. Each of these frames was analysed with both the traditional defect counting method and the two proposed topological order parameter methods. In the following sections we outline the procedure by which each of these tools was used.

Defect counting

Defect counting was performed using the in-built routine provided by DLPOLY 4.[23] The configuration in each of the recorded frames (2-501) was compared with the initial undamaged

configuration (frame 1). In general, a particle may leave its original atomic site creating a vacancy. If the final position of this particle lies within a fixed distance of an atomic site occupied by another atom, an interstitial defect results. The site-interstitial cutoff distance was selected equal to 1.8 Å, corresponding to half of the mean Ar-Ar bond distance. Antisite defects are not distinguished by the DLPOLY 4 defect counting routine.

A particle is considered to be a member of the set of "damaged" particles i.e a defect, if the displacement from its original undamaged crystalline position exceeds 50% of the value of the shortest bond-length of the system. The shortest "bond length" can be obtained from the radial distribution function. The partial radial distribution function for a pair of atomic

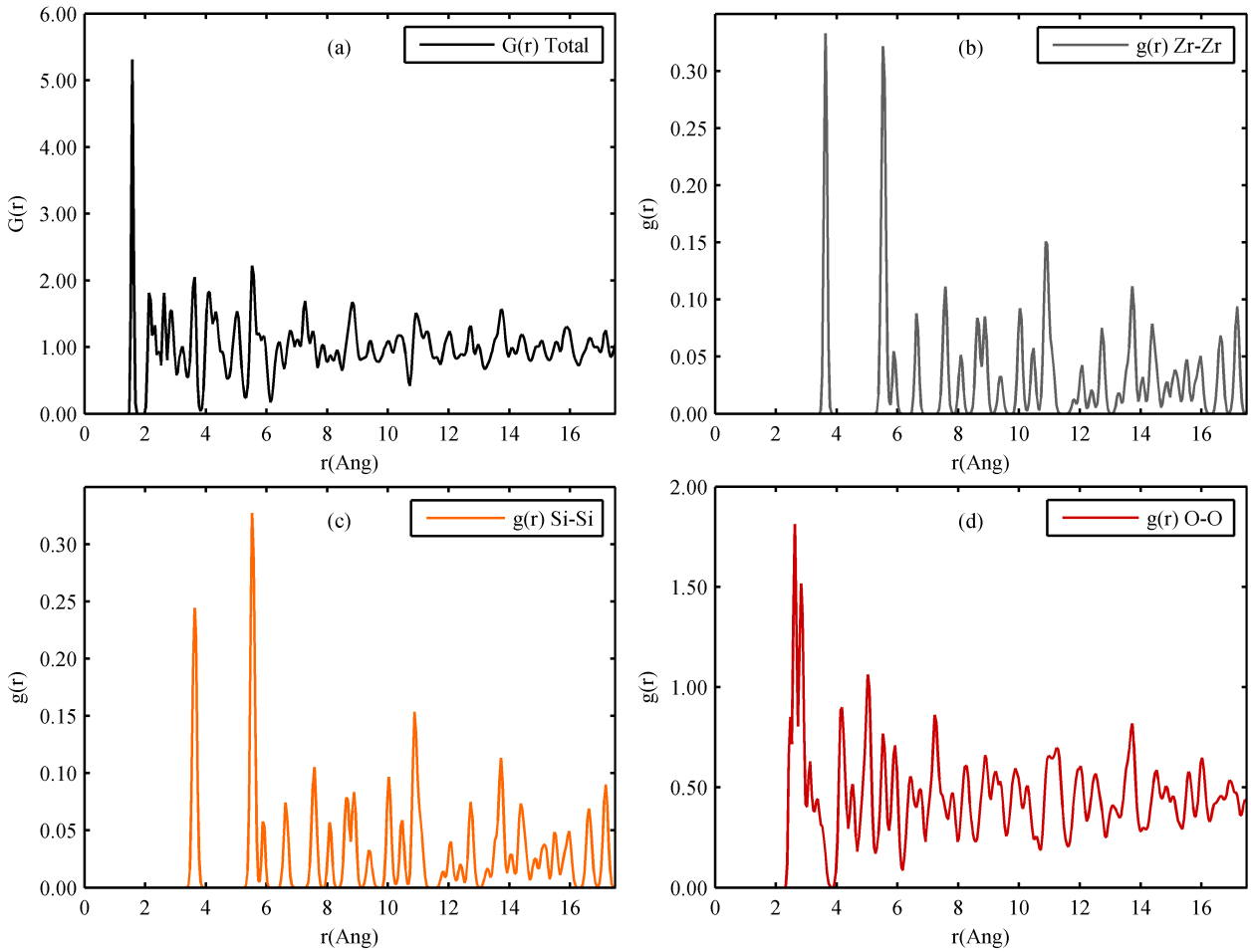

Figure 1: Total radial distribution function (1.a) and partial radial distribution functions for the Zr-Zr (1.b), Si-Si pairs (1.c), O-O pairs (1.d).

sites of species α and β is defined as:

$$g_{\alpha\beta}(r) = \frac{V}{n_\alpha n_\beta} \sum_{i}^{n_\alpha} \sum_{j \neq i}^{n_\beta} \langle \delta(r - r_{ij}) \rangle, \tag{18}$$

where V is the system volume, n_α and n_β are the respective number of atoms of type α and β. The total radial distribution function, is obtained from:

$$G(r) = \sum_{\alpha} \sum_{\beta} g_{\alpha\beta}(r). \tag{19}$$

Radial distribution functions for pristine (undamaged) zircon are shown in Figure 1. The first maximum in $G(r)$ (Figure 1.a) occurs at a distance of 1.55 Å and so we set the "damage distance", $r_d = 0.75$ Å, which is a little less than half this value. For the LJ system, the position of the first maximum in $G(r)$ is at 3.78 Å. Initially we tried a value of $r_d = 1.85$ Å for this system of and so the damage distance is selected equal to 1.85 Å. However, we had to modify this distance to the lower value of 1.75 Å after trial runs led to the observation of multiple occupancy of atomic sites (two or more atoms were simultaneously found in the same atomic site).

Order parameters

To properly characterize the damage from a recoil cascade event, we have calculated species-specific Steinhardt and Hermite order parameters. The method for doing this is as follows:

The zircon structure was separated into three substructures, each containing only atoms of the same type. For each of these substructures, a list of the nearest neighbors for every reference particle was constructed, by using the position of the first minimum of the respective partial $g(r)$ as a cutoff distance. Two particles A and B are considered to be bonded if the distance r_{AB} between them is shorter that the first minimum of both the partial radial distribution function $g_{AB}(r)$ and the total radial distribution function $G(r)$. SOP were

calculated for $0 < \ell \leq 10$, while HOP were obtained for $0 < n \leq 16$, for each of the 500 frames. The algorithm for computing these order parameters consisted of the following steps: (1) An atom is chosen in one of the configurations - the reference atom; (2) distances and angles are obtained for each of the near neighbors of the reference atom and used to compute the SOPs and HOPs. (3) The procedure is repeated until every atom has been selected as the reference atom.

For the initial undamaged structure, the average value of SOP and HOP is calculated. Then for each damaged frame, the number of particles with a SOP/HOP value above the average, $n_g(t)$, is calculated and compared with the respective number $n_g(0)$ in the initial structure. Finally, the number of particles: $n_h(t)$, with SOP/HOP increased values when compared with the respective values in the reference frame is calculated.

Extra care is needed when handling periodic boundaries. Since the analysis was performed using the output file of the simulation, to avoid overcounting the number of damaged particles, atoms that travel through the boundaries of the simulation box are identified during the analysis and their positions are fixed to be the same as in the initial undamaged structure.

During the analysis, when identifying nearest neighbors, the minimum image convention method was not applied. Instead, the initial undamaged structure was replicated 3 times in each spatial dimension (27 replicas in total). For the analysis of the damaged structure, only the positions of the atoms that lie within the original cell are updated. For the creation of the neighbor list, it is necessary to calculate the distances between all the particles of the substructure. To decrease the calculation time, the replicated supercell was truncated to include only replicated atoms that lie within a distance less than the first minimum of the partial RDF from the surface atoms.

Additionally, to avoid identifying as damaged a particle that simply undergoes thermal vibration, a special condition is applied in the calculation of SOP/HOP. For each reference particle, the distances r_{ij} with all the nearest neighbours are calculated for each of the frames.

The difference $d_{ij}(t_n) = |r_{ij}(t_n) - r_{ij}(0)|$ of the distance r_{ij} between each damaged frame (labeled as time t_n) and the reference frame ($t = 0$) is calculated. The process is depicted in Figure 2. To characterize a particle as a possibly damaged particle, we require at least one of the distance differences, d_{ij}, to be greater than the distance r_d. If none of these satisfy the condition, SOP/HOP values for the specific reference particle are set to the values calculated for the same particle in the initial undamaged frame.

This method does not automatically characterize a particle as damaged. If $d_{ij}(t_n) > r_d$, then when particle j is used as reference particle it will also be $d_{ji}(t_n) > r_d$. This way, the SOP/HOP values of both particles will be affected, classifying both particles damaged when only one of the pair may be so. To avoid erroneous estimation of the number of damaged particles, a correlation between the actual number of damaged particles and the numbers $n_g(t)$ and $n_h(t)$ is performed. In the initial undamaged substructure for each species, a number of particles, equal to 10% of the total number of particles in the substructure, are deliberately displaced from their initial positions by a distance $R > r_d$ to create an artificially damaged structure. The quantities: $n_g(t)$ and $n_h(t)$ are calculated for this case and are compared with the number of deliberately damaged particles. To increase the accuracy of the correlation, this step is repeated 100 times and the number of damaged particles is compared with the average $n_g(t)$ and $n_h(t)$ values.

For amorphous materials, because of the diffusion, it is not safe to create deliberately damaged structures by using only the initial undamaged one. Instead, we equilibrate the reference structure for 50k timesteps using NVT dynamics to create 500 deliberately damaged structures, every 100 steps, by using the output file of the simulation. We used each of these frames to find the correlation between the actual number of damaged particles and the numbers $n_g(t)$ and $n_h(t)$.

Not all Q_ℓ and $\langle\widetilde{\psi}_n(r)\rangle$ give a satisfactory estimation of the number of damaged particles, requiring a sifting process, conducted as follows: First, the average values of SOP/HOP values are plotted as a function of time. From these curves, only the values of ℓ and n

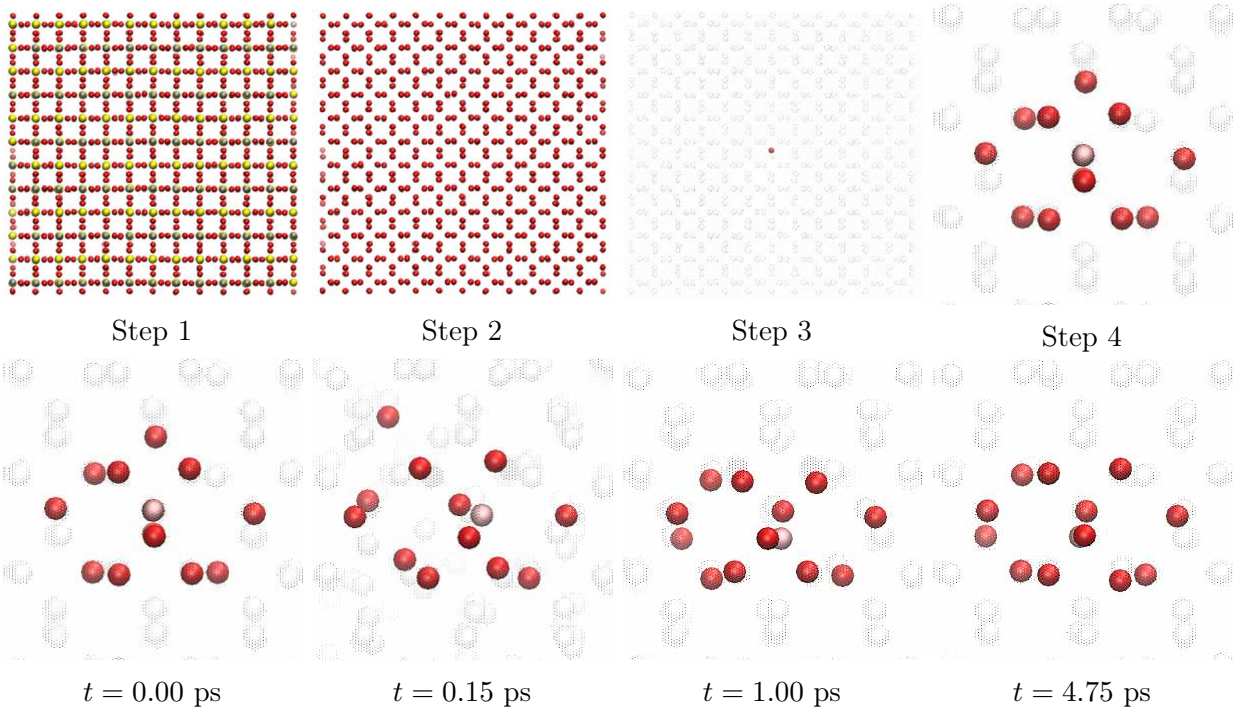

Figure 2: The process of the SOP/HPP calculation. From the initial undamaged structure (step 1), a substructure is created by selecting the atoms of a single species (here the oxygen atoms, step 2). A reference particle is selected (step 3) and its nearest neighbours are identified (step 4). This "local" structure is observed during the total time of the simulation and the SOP/HPP are calculated for each frame.

which have the expected qualitative behaviour are selected. For these values, we calculate correlation coefficients between the number of deliberately damaged particles and the number of particles $n_h(t)$. For example, for the zirconium atoms it was found that for 86 deliberately displaced atoms, $n_h(t)$ receives an average value of 35.13. For the actual damaged structure, the number of damaged particles is obtained using the formula

$$n_d(t) = \frac{86}{35.13} n_h(t). \tag{20}$$

Some of the selected values of ℓ, n can give rise to negative values for the number of damaged particles because $n_g(t) < n_g(0)$. These members of the set were subsequently discarded. The number of damaged particles estimated for the different selected ℓ, n values are then averaged to calculate the actual number of damaged particles.

Results

Radiation damage in crystalline zircon

The damaged zircon crystal was analysed using both defect counting and the proposed topological methods in order to demonstrate the accuracy of the latter.

Defect counting

Figure 3 shows the actual number of damaged particles for the three different species (Zr, Si and O) for zircon as determined using the inbuilt defect counting algorithm in DLPOLY 4 (Wigner-Seitz method). In each case, the number of damaged atoms rises to a maximum in a time ~ 0.25 ps, before falling again and then reaching a plateu at ~ 1 ps. The greatest number of damaged particles are O species, with a peak damage value of 111 atoms. The respective values for the silicon and zirconium species are 39 and 25.

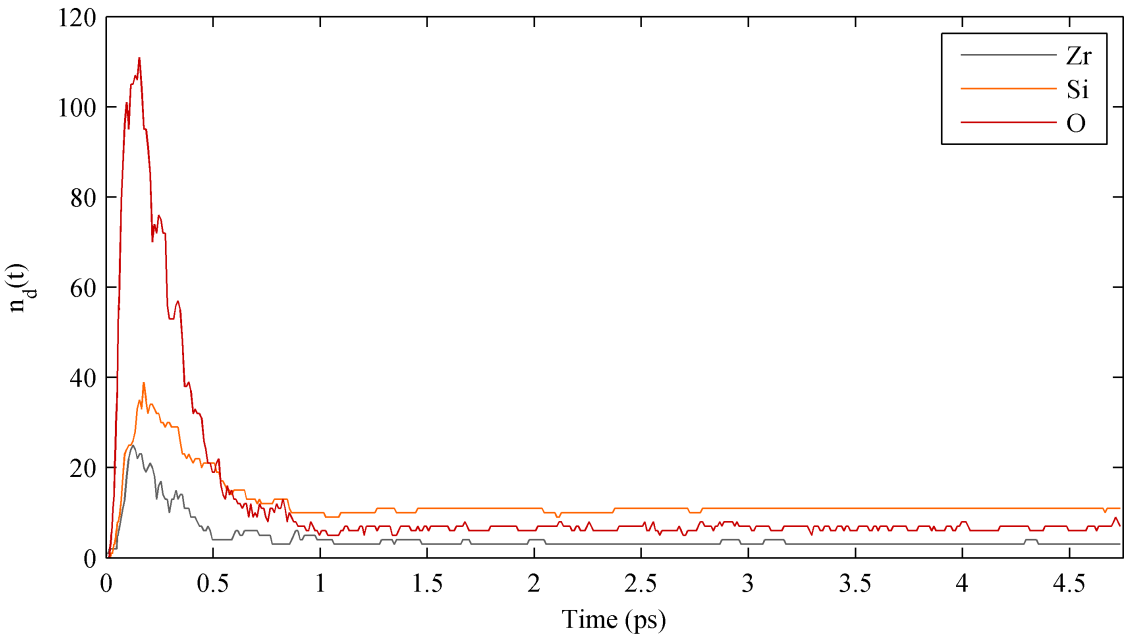

Figure 3: Plot of the time evolution of defects in the zircon crystal and for the different species as calculated by the DLPOLY 4 in-built routine.

Steinhardt order parameters

The curves showing the number of damaged particles as calculated using the defect counting method, follow the characteristic damage-like pattern shown in figure 3. Regardless of whether the material is crystalline or not, it is expected that the number of damaged particles will follow a similar pattern. The only differences are expected at the rate at which the number of damaged particles are increasing at the beginning of the simulation and also at the recovery stage which will define the number of particles that will form the plateau. Since our effort is to correlate the SOP values with the number of damaged particles, we assume that the evolution of SOP must follow a similar pattern.

For the zircon system, the time evolution of the majority of SOP follows a rather arbitrary pattern. However, by comparing with the time evolution of the number of defects, it is found that for some values of ℓ the evolution of the SOP exhibits a "desired behaviour", by reaching a maximum value at the time of maximum damage and forming a plateau starting at $0.5 < t < 1$ ps. For the zirconium and silicon atoms, Q_1, Q_6 and Q_9 demonstrated a damage-like evolution, as shown in figure 4, while for the oxygen atoms it was Q_9 and Q_{10}. It can be argued that the evolution of these SOP values is directly related to the number of defects of the system. The calculated number of damaged particles using SOP method for each of the three ℓ values were averaged and the result gave good agreement with the number of defects calculated by the Wigner-Seitz method for both the zirconium and silicon atoms (Figures 5 and 6), especially in the recovered crystal. For the oxygen atoms however (Figure 7) there is a strong disagreement in the recovery region. However this can be explained by the fact DLPOLY defect counting routine cannot identify antisites, which are quite numerous.

A simple way to estimate the number of total defects for each species, is to find for each of the damaged frames the number of atoms that are displaced by $r > r_d$. The total number of oxygen defects is plotted in Figure 7. As can be seen, the total number of oxygen defects in the equilibrium region is still lower in comparison with the number estimated with the SOP method, but the difference is much smaller. A possible solution is to use even

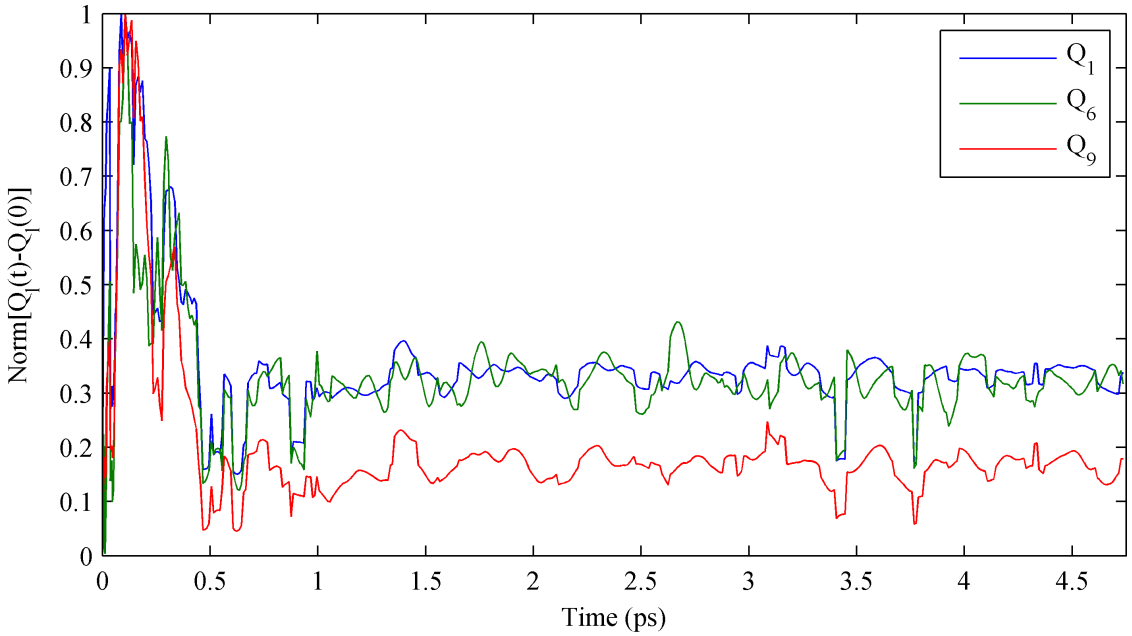

Figure 4: The time evolution of Q_1, Q_6 and Q_9 for the zirconium species. The plot demonstrates the values of $Q_l(t) - Q_l(0)$ normalized to give unit maxima. These three was the only SOP that presented a damaged-like behavior.

higher order SOP in order to have the ability to average the number of estimated damage particles for even more ℓ values and get a better statistical distribution, but this will have a computational cost. To compute SOP up to $\ell = 16$, the computational time becomes 2.4 times higher and 5.2 times for values up to $\ell = 24$. However, since in amorphous materials there are no antisites, we expect that the SOP method will give an excellent account of the number of damage particles, as in the case of zirconium and silicon atoms of the zircon crystal.

Hermite order parameters

For the zircon atoms $\langle\widetilde{\psi}_9(r)\rangle$, $\langle\widetilde{\psi}_{10}(r)\rangle$, $\langle\widetilde{\psi}_{11}(r)\rangle$, $\langle\widetilde{\psi}_{12}(r)\rangle$, $\langle\widetilde{\psi}_{14}(r)\rangle$ and $\langle\widetilde{\psi}_{15}(r)\rangle$ demonstrated a damage-like evolution with time while for silicon atoms $\langle\widetilde{\psi}_{10}(r)\rangle$, $\langle\widetilde{\psi}_{11}(r)\rangle$, $\langle\widetilde{\psi}_{14}(r)\rangle$ and $\langle\widetilde{\psi}_{15}(r)\rangle$ were used. For the oxygen atoms, only $\langle\widetilde{\psi}_2(r)\rangle$ demonstrated the desired behavior. The results obtained with HOP method for zircon and silicon (Figures 5 and 6) show very good correlation with the results obtained with both Wigner-Seitz and SOP methods, which

can be regarded as a self-validation of the two proposed methods in the case where there are no antisites in the system. There seems to be a small overestimation of the maximum damage for the silicon and oxygen atoms. This problem can be solved by modifying the criteria under which the method identifies a damaged particle, in order to take into account not only the distance between the nearest neighbours, but also the local geometry.

For both SOP and HOP methods, the results show a clear correlation between the number $n_g(t)$ and the actual number of damaged particles $n_d(t)$ as calculated using the traditional defect counting method provided by the DLPOLY 4 in-built defect calculation routine. The fact that the results obtained with SOP and HOP methods converge is very important in cases were the defect counting method is not applicable or erroneous, as for amorphous materials. We can use both methods to calculate the number of damaged particles $n_d(t)$ and estimate the accuracy of the results by checking if they converge to the same values.

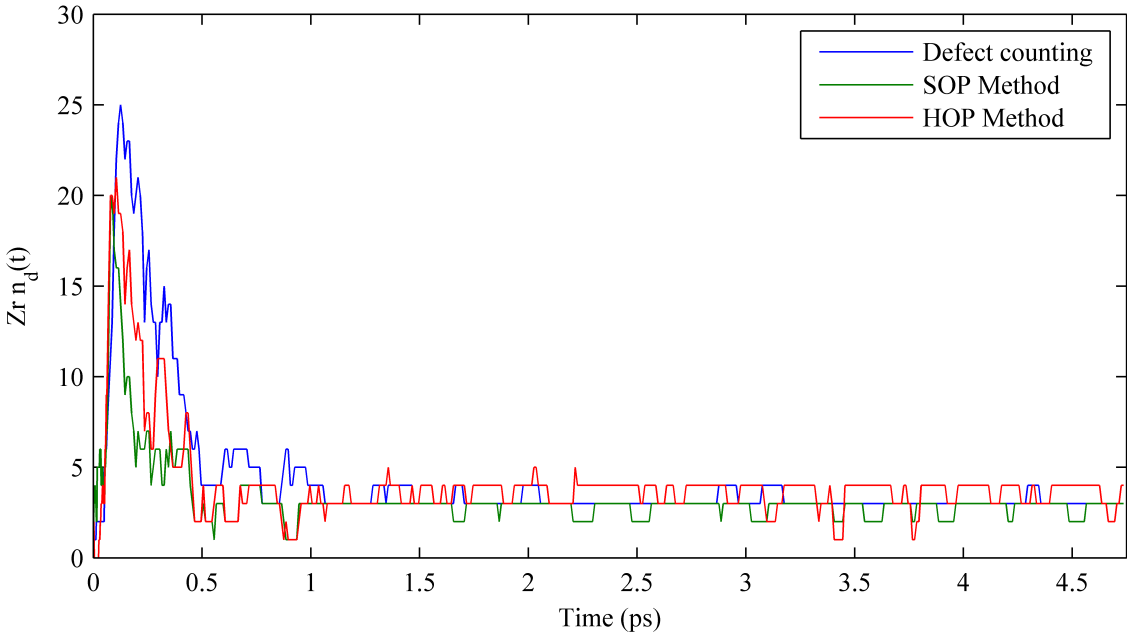

Figure 5: Comparison between the number of defects of the zirconium atoms calculated using Wigner-Seitz method and the number of zirconium damaged particles calculated using SOP and HOP methods.

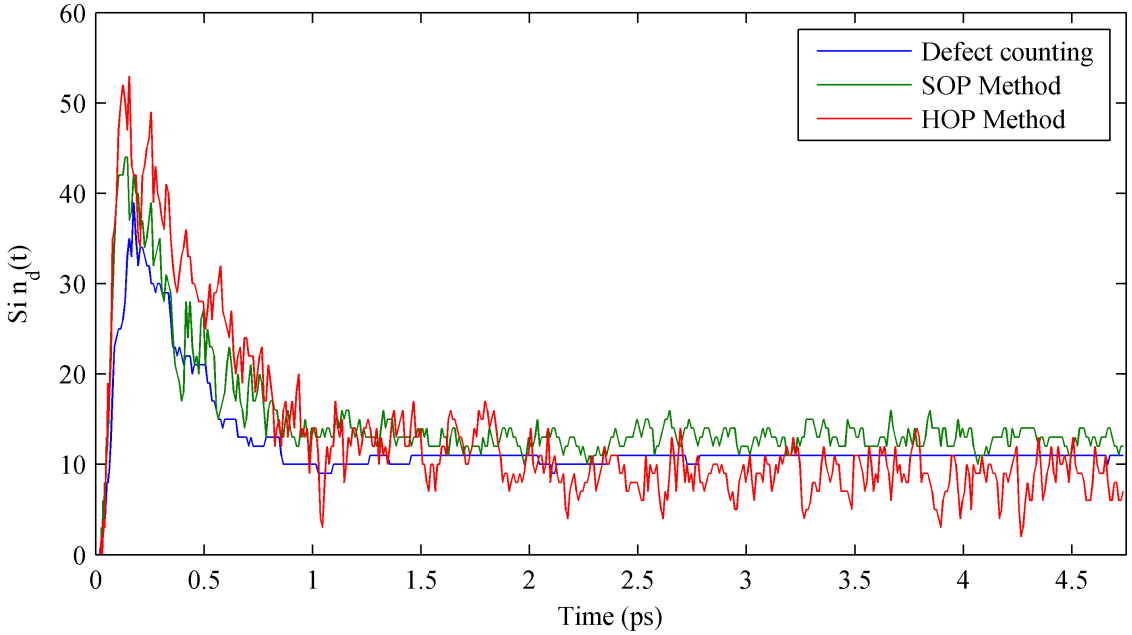

Figure 6: Comparison between the number of defects of the silicon atoms calculated using Wigner-Seitz method and the number of zirconium damaged particles calculated using SOP and HOP methods.

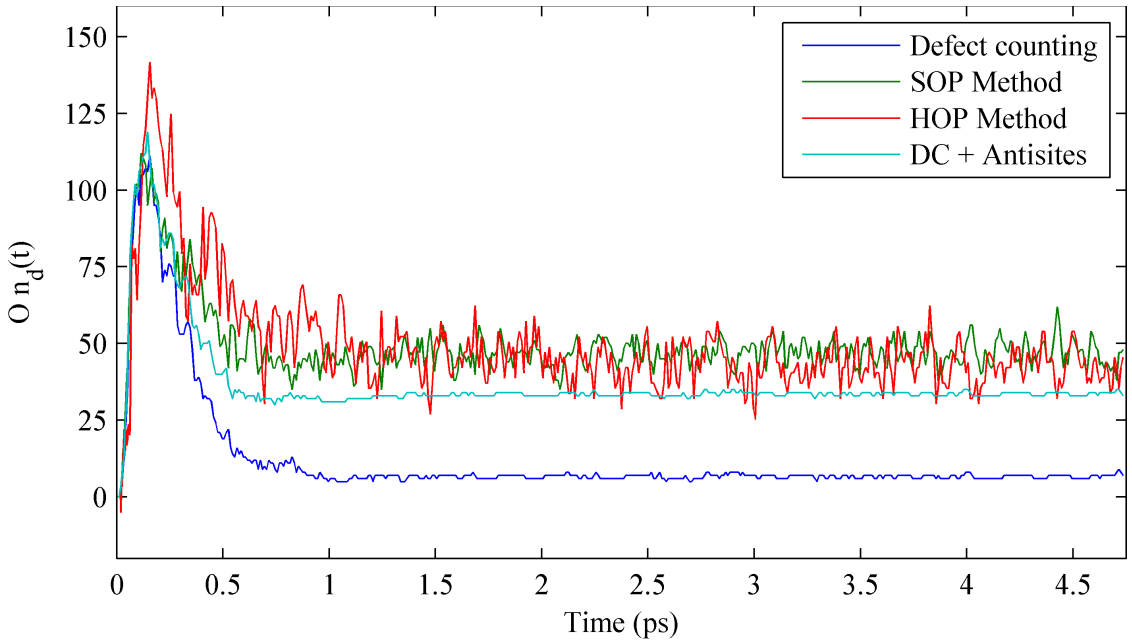

Figure 7: Comparison between the number of defects of the oxygen atoms calculated using Wigner-Seitz method and the number of oxygen damaged particles calculated using SOP method. The light blue line corresponds to the total number of displaced oxygen atoms: damaged particles and antisites.

Radiation damage in Lennard Jones glass

The traditional defect counting method shows a steadily increasing number of damaged particles in the glass for the radiation damaged structure and for the first 1.5 ps of the simulation and then a recovery is observed (Figure 8). The final number of damaged particles is estimated around 800. However, since we have an amorphous material we expect the defect counting method to overestimate the damage at the end of the simulation. In amorphous materials, there are no point defects - instead we have bond defects. There is the possibility that because of the damage and the diffusion observed in amorphous materials, a local cluster of particles to move all together or rotate around an axis or both, making all the particles to be displaced from their initial positions by more than r_d, but without breaking any bonds. While there is no damage in this cluster, the Wigner-Seitz method will identify all the particles of the cluster as false-positive damaged particles.

The SOP/HOP methods on the other hand, do not use the initial structure to identify the number of damaged particles - they only use the local environment of each particle. The damage is estimated based on the alterations of this local structure. Additionally, the fact that a correlation map is generated from an equivalent equilibrium structure makes this method immune to the effect of diffusion. Using Q_5, Q_8 and $\langle\widetilde{\psi}_{13}(r)\rangle$ for the SOP and HOP methods respectively and as argued above, the SOP/HOP method estimates a significantly lower number of damaged particles at the end of the simulation (Figure 8). However, the SOP method seems to overestimate the damage at the initial stages of the simulation. This fact can also be explained based on how a damaged particle is defined in amorphous materials. Although there is not a perfect correlation between the two proposed methods, the results are reasonably close and suggest a correct estimation of the number of damaged particles.

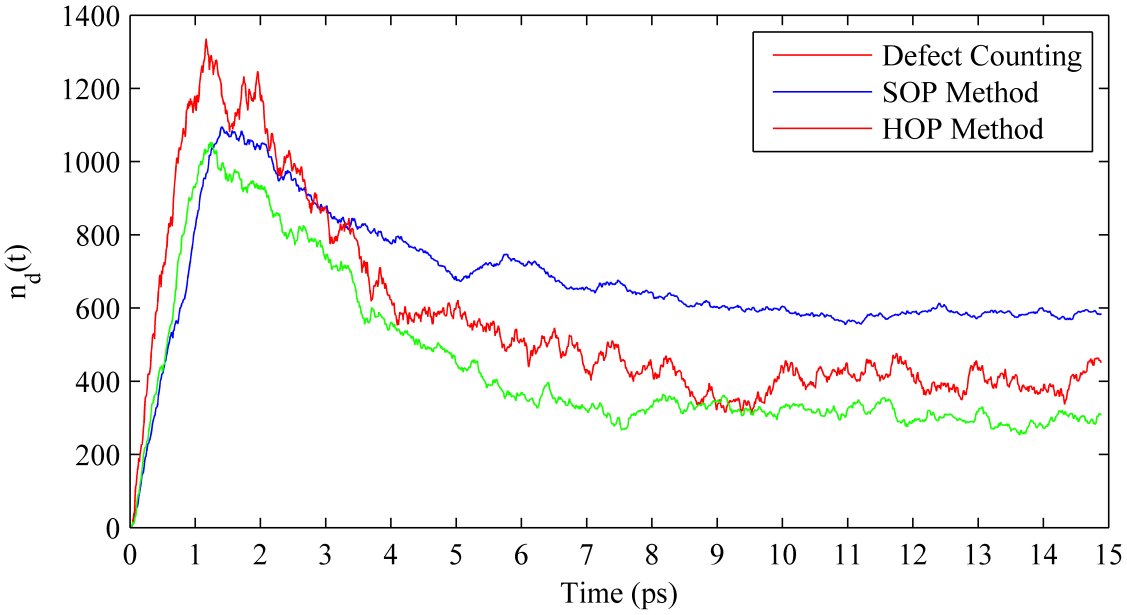

Figure 8: The evolution of radiation damage in a simple Lennard-Jones system, calculated with the traditional Wigner-Seitz method and with the two proposed topological methods.

Discussion and conclusions

We have developed two different topological methods to characterize the radiation damage effects in amorphous materials, based on Steinhardt order parameters and Hermite polynomial parameters. These method were tested on a zircon system to estimate the number of damaged particles for each species separately. The results obtained with both methods are consistent with the simple defect counting technique based on the Wigner-Seitz method, in case there are no antisites in the system. For systems with antisite defects, the SOP method seems to overestimate the damage at the recovery stage. When applied to a simple Lennard-Jones system, SOP and HPP methods estimate a higher number of damaged particles for the initial stages of the damage simulation and a lower number in the recovery region, which can be explained using reasonable arguments based on the nature of the damage in amorphous materials.

Although these new topological methods could be improved in order to be consistent for all systems - including structures with antisite defects - they show great potential towards radiation damage characterization in amorphous materials. Current and future develop-

ments of the method will be able to give accurate information regarding the extent and the mechanism of the damage in both global and local level.

References

(1) Hobbs, L. W. In *Engineering of Crystalline Materials Properties: State of the Art in Modeling, Design and Applications*; Novoa, J. J., Braga, D., Addadi, L., Eds.; Springer Netherlands: Dordrecht, 2008; Chapter Topological Approaches to the Structure of Crystalline and Amorphous Atom Assemblies, pp 193–230.

(2) Archer, A.; Foxhall, H. R.; Allan, N. L.; Gunn, D. S.; Hardind, J. H.; Todorov, I. T.; Travis, K. P.; Purton, J. A. *Journal of Physics: Condensed Matter* **2014**, *26*, 485011.

(3) Guttman, L. *Journal of non-crystalline solids* **1990**, *116*, 145–147.

(4) Hobbs, L. W.; Sreeram, A.; Jesurum, C. E.; Berger, B. *Nuclear Instruments and Methods in Physics Research B: Beam Interaction with Materials and Atoms* **1996**, *116*.

(5) Hobbs, L. W.; Jesurum, C. E.; Pulim, V.; Berger, B. *Philos. Mag. A* **1998**, *78*.

(6) Yuan, X.; Hobbs, L. W. *Nuclear Instruments and Methods in Physics Research Section B: Beam Interactions with Materials and Atoms* **2002**, *191*, 74 – 82.

(7) Dewan, L.; Hobbs, L. W.; Delaye, J.-M. Modeling Radiation-Induced Alteration of the Network Structure of Alkali Borosilicate High-level Waste Glass. MRS Online Proceedings Library Archive. 2011; p 1298.

(8) Dewan, L.; Hobbs, L. W.; Delaye, J.-M. *Journal of Non-Crystalline Solids* **2012**, *358*, 3427 – 3432, Glasses for Energy.

(9) Krishnan, N. M. A.; Wang, B.; Yu, Y.; Le Pape, Y.; Sant, G.; Bauchy, M. *Phys. Rev. X* **2017**, *7*, 031019.

(10) Krishnan, N. M. A.; Wang, B.; Pape, Y. L.; Sant, G.; Bauchy, M. *The Journal of Chemical Physics* **2017**, *146*, 204502.

(11) Hobbs, L. W. *Journal of Non-Crystalline Solids* **1995**, *182*, 27 – 39.

(12) Thorpe, M.; Jacobs, D.; Chubynsky, N.; Rader, A. In *Rigidity Theory and Applications*; Thorpe, M. F., Duxbury, P. M., Eds.; Springer US: Boston, MA, 2002; pp 239–277.

(13) Foxhall, H.; Travis, K.; Hobbs, L.; Rich, S.; Owens, S. *Philosophical Magazine* **2013**, *93*, 328–355.

(14) Wang, B.; Krishnan, N. M. A.; Yu, Y.; Wang, M.; Pape, Y. L.; Sant, G.; Bauchy, M. *Journal of Non-Crystalline Solids* **2017**, *463*, 25 – 30.

(15) Baranyai, A.; Puszta, L.; Ruff, I. *Electrochemical Acta* **1988**, *33*, 1229–1234.

(16) Lechner, W.; Dellago, C. *The Journal of Chemical Physics* **2008**, *129*, 1–5.

(17) Reinhardt, A.; Doye, J. P. K.; Noya, E. G.; Vega, C. *Journal of Chemical Physics* **2012**, *137*.

(18) Steinhardt, P. J.; Nelson, D. R.; Ronchetti, M. *Phys. Rev. B* **1983**, *28*, 784–805.

(19) Trachenko, K. O.; Dove, M. T.; Salje, E. K. H. *Atomistic modeling of radiation damage in zircon* **2001**, 1947–1959.

(20) Trachenko, K. O.; Dove, M. T.; Geisler, I.; Todorov, I. T.; Simth, B. *Radiation damage effects and percolation theory,* **2004**, 2623–2627.

(21) Trachenko, K. O.; Zarkadoulia, E.; Todorov, I. T.; Dove, M. T.; J., D. D.; Nordlund, K. *Nuclear Instruments and Methods in Physics Research* **2012**, *B*, 6–13.

(22) Devanathan, R.; Corrales, L. R.; Weber, W. J. *Physical Review* **2004**, *B*, 1–9.

(23) Todorov, I. T.; Smith, W.; Trachenko, K.; Dove, M. T. *Journal of Materials Chemistry* **2006**, *16*, 1911–1918.

(24) Gale, J. D. *The Journal of Chemical Society, Faraday Transactions* **1997**, *93*, 629–637.

(25) Ziegler, J.; Biersack, J. P.; Littmark, U. In *Treatise on Heavy-Ion Science: Volume 6: Astrophysics, Chemistry, and Condensed Matter*; Bromley, D. A., Ed.; Springer US: Boston, 1985; Vol. 1.

(26) Rahman, A.; Mandel, M. J.; McTague, J. P. *Journal of Chemical Physics* **1976**, *64*, 1564–1568.